Synthesis Gold Nanoparticles by Plasma Jet as Different Diameters of System

Maryam Ali Raheem[1*] iD ✉ **and Ban H. Adil[2]** iD ✉

[1,2]Department of Physics, College of Sciences for Women, University of Baghdad, Baghdad, Iraq.
*Corresponding author.

Abstract

In this work, gold nanoparticles (AuNPs) were created utilizing a plasma jet method and 0.5 gm/mol of gold salts ($4H_2O \cdot HAuCl_4$) with varied flow diameters (0.6 mm, 0.8 mm, 1 mm, and 1.2 mm). The gas flow changes according to the system diameter (2,2.4,3.4, and 3.6 L/min, respectively). X-ray diffraction, ultraviolet, visible spectra, and FESEM were each used to investigate the nanoparticles. The XRD pattern revealed that the film's extreme peaks reflect crystallinity, with an average crystallite size of (18–26) nm and a face-centered cubic structure. The surface plasmon resonance for colloidal AuNPs produced in the UV was at 536–540 nm.A field emission scanning electron microscope (FESEM) was used to look at the morphology of the Au NPs. The round particles ranged in size from (38-65) nm. The findings of this work provide encouraging evidence for the straightforward and inexpensive production of nanomaterials with various dimensions.

Keywords: Plasma jet, Ar gas, AuNPs, XRD, FE-SEM.

1. Introduction

The nano-science and its techniques have been categorized as interdisciplinary sciences of substantial relevance in numerous disciplines because of their large surface area, perfect comparative characteristics with low density, strong surface contact, and diversified methodology [1]. One definition of a nanoparticle is an extremely tiny particle with a size between 1 and 100 nm [2]. Through biological, physical, and chemical processes, these nanoparticles can be created. One of the distinctive characteristics of metallic nanoparticles is surface Plasmon resonance [3–6]. Because of characteristics like its excellent thermal conductivity, amazing resistance to oxidation, and antimicrobial activity, nanotechnology is viewed as an essential and future-proof technology. It could advance the study of biology, engineering, medicine, and physics [7–8]. Magnetic, optical, electrical, and storage technologies can all benefit from the use of nanoparticles [9]. Due to its unique properties of being inert, biocompatible, and notably low toxicity, gold (AuNPs), one of the most significant nanoparticles, has been extensively employed for both medical and non-medical reasons [10]. As a result, they have been applied to implants, cosmetics, medical device coatings, food preservatives, medical equipment, and dental resin composites. Gold (Au) and other noble metal NPs have demonstrated potent and long-lasting antibacterial activity against a variety of microbes [11]. As a quasi-neutral gas made up of charged and neutral particles that interact with one another, plasma, the

fourth state of matter, can also be considered. 99% of the substance in the cosmos is made up of plasma, which is made up of electrified gases made of separated positive ions and negative electrons of atoms. Gaseous nebulae, star interiors, interstellar hydrogen, and atmospheres all include plasma [12]. Based on the temperature of the electrons with respect to the other particles (ions and neutral particles), there are two forms of plasma: thermal and non-thermal. In thermal plasma, the electron temperature and the temperature of the heavier particles are practically equal (they are in thermal equilibrium). In non-thermal plasma, however, the electron temperature is significantly higher and the heavier particles are essentially at room temperature. The goal temperature of conventional thermal plasma is greater than 3000 °C, making it ideal for mineralogy but unsuitable for treating live tissue [13]. The application site temperature of cold plasma, also known as non-thermal plasma, is less than 40 °C, making it appropriate for treating live tissue [14–16]. Due to its inherent benefits over methods for producing solid, liquid, and gas phases, plasma technology is now exploited as a generation method for nanomaterials. The use of plasmas and nanoparticles in biological applications reveals several synergistic effects and effective therapeutic results [17–20]. The aim of this study is to examine how the diameters of plasma jets affect the prepared nanoparticle properties to choose the best outcomes for additional applications.

2. Materials and Methods
2.1 Preparation of the Solution
   In this investigation, 99% pure gold salts (4H2O•HAuCl4) with a molecular weight of 0.5 g/mol were used. Equation (1) below is then used to get the required weight:

Concentration (mole) = (mass(g))/(Molecular weight (g/mol)*volume (litter)) [18]   (1)

2.2 Preparation of nanoparticles
   The following steps are taken to prepare the AuNPs: The solution will be created with a 0.5 mM concentration of (4H2O•HAuCl4) gold salts in the desired sizes, and the prepared form will be put on a holder within the metal tube as instructed in the details. For the flow of Ar gas, the metal tube is placed vertically in the catcher at [0.6 mm, 0.8 mm, 1 mm, 1.2 mm]. Depending on the system's diameter, the gas flow varies (2,2.4, 3.4.6, and L/min, respectively). A 1cm gap existed between the liquid surface and the circular metal tube's tip on the beaker; such that there was a 1mm separation between the liquid surface and the nozzle. Furthermore, the 5-minute plasma exposure duration with a sample gas flow was used to regulate the Argon gas supplied in metal tubes. As seen in **Figure 1**, the value corresponding to the system's provided voltage quickly increased as plasma developed between the liquid's surface and the tube (1). The purpose of this study was to determine the effect of the diameters of the system. To obtain the best results, all diameters produced plasma, where 1mm was more efficient to produce nanomaterials:
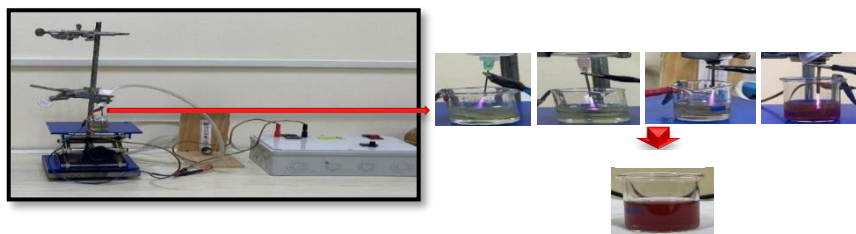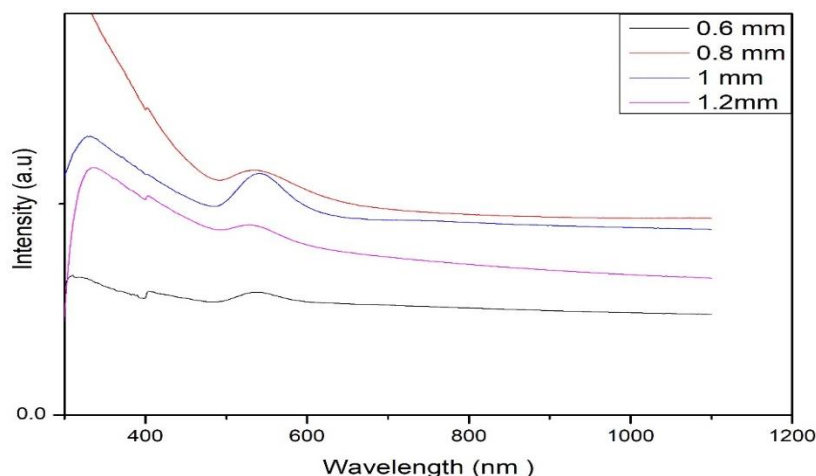

Figure 1. Illustrates the plasma jet system syntheses AuNPs as a different diameter
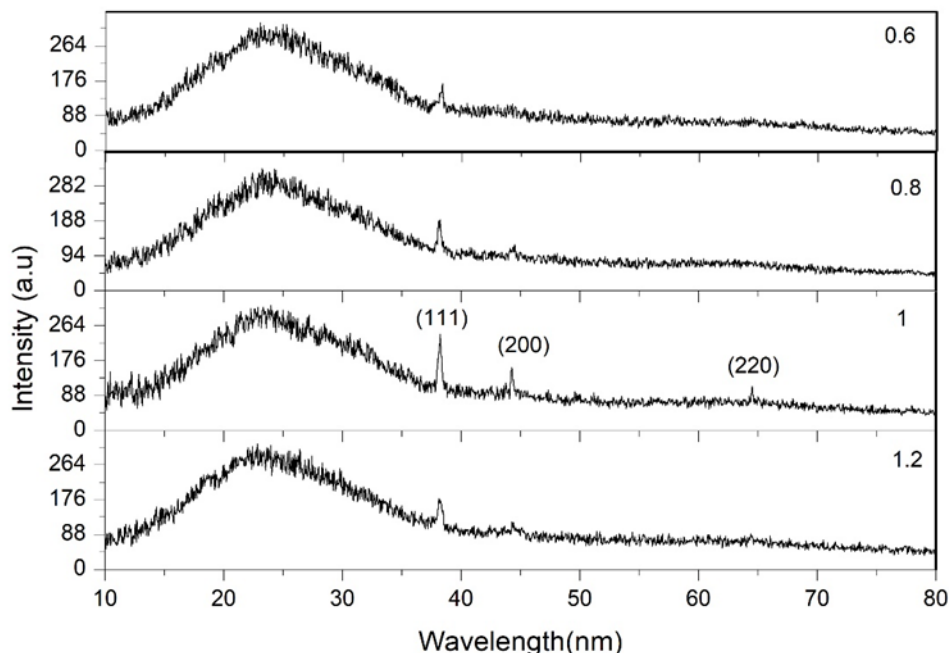
3. Results

3.1 Absorption Spectra

In **Figure 2**, the absorption spectra of AuNPs for different diameters (0.6, 0.8, 1, and 1.2) mm are displayed. The maximum absorption occurred between 536 and 540 nm, and the crystal size was in the range of nanometers (1-100) nm. Compared to other samples, the sample created at 1 mm had the lowest particle size, and AuNPs made at this size showed enhanced absorbance and a blue-shifted absorbance spectrum. The results show the presence of spherical-shaped Au nanoparticles and are in excellent agreement with those discovered in the literature to model the light scattering spectra of Au nanoparticles using Mie theory.

Figure 2. Illustrates the plasma jet system syntheses AuNPs as a different diameter

### 3.2 The Results of X-Ray Diffraction

The crystallinity of artificial AuNPs produced by cold plasma at different diameters (0.6, 0.8, 1, and 1.2 mm) was investigated using the X-ray diffraction (XRD) technique. **Figure 3** presents the results. The best results were obtained at 1 mm, when three peaks appeared at peaks at 2 = 38.1, 44.3, and 64.5. The behavior of Au NPs varied depending on the diameter of the probe. All three peaks shared the (111), (200), and (220) conventional Bragg reflections of the face center cubic (fcc) lattice. The severe diffraction at peak 38.1 shows that the direction (111) was fixed as the preferred growth orientation for zero-valent gold if the sample prep is 0.6 mm and there is just one peak at 2 = 38.1. This depicts solids that are the size of molecules and are composed of recurring 3D patterns of identically spaced atoms or molecules. This XRD pattern is frequently seen in pure Au nanocrystals [22]. The Debye-Scherrer equation was used to regulate the sample crystal size. The crystal diameters of the generated samples varied between (18 and 26 nm), depending on the diameter of the electrode, in agreement with other results [18].

Figure 3. X-ray patterns of AuNPs as a function of probe diameters

3.3 The Results of FE-SEM

FESEM was used to analyze the shape of AuNPs generated by atmospheric plasma at an electrode diameter of 1 mm. The nanoparticles in **Figure 4** are seen in a FESEM picture to have a spherical form, along with another particle that resembles a spotlight. It was discovered that the particle sizes varied from 30 to 33 nm. It is well known that a nanoparticle's shape has a substantial impact on both its optical and electrical capabilities [21].
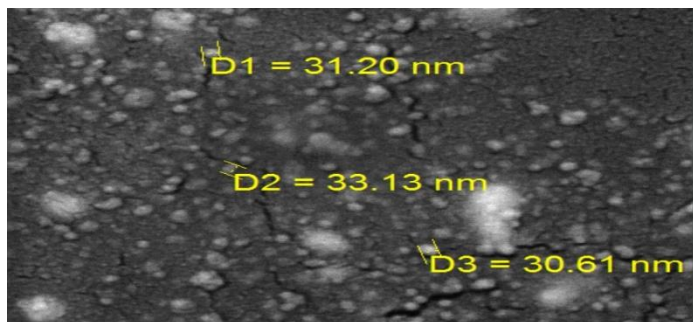
Figure 4. FESEM of AuNPs prepared using a cold plasma technique plasma jet

4. Conclusion

High-density data storage is one of the unique skills that gold nanoparticles have found in a number of scientific fields. With the use of a UV-vis-NIR spectrophotometer and transmission electron microscopy, gold nanoparticles made by a plasma jet have been examined. Growing applications of nanoparticles, particularly metallic nanoparticles, show how important this topic is today. One of the most useful metallic nanoparticles is the gold particle. The findings of this work

provide encouraging evidence for the straightforward and inexpensive production of nanomaterials with various dimensions.

Conflict of interest

The authors declare that they have no conflict of interest.

Ethical approval

This article does not contain any studies with human participants or animals performed by any of the authors.

References

1. Abdullah, Q.; Obaid, A.; Bououdina, M. Influence of gas carrier on morphological and optical properties of nanostructured In2O3 grown by solid-vapor process. *Ceramics International* **2018**, *44*, 4699-4703. https://doi.org/10.1016/J.CERAMINT.2017.12.051.
2. Nakamura, S.; Sato, M.; Sato, Y.; Ando, N.; Takayama, T.; Fujita, M.; Ishihara, M. Synthesis and application of silver nanoparticles (Ag NPs) for the prevention of infection in healthcare workers. *International journal of molecular sciences* **2019**, *20*(*15*), 23-34.https://doi.org/10.3390 /ijms20153620.
3. Rakaa, J.; Obaid, A.S. Preparation of Nanoparticles in an Eco-friendly Method using Thyme Leaf Extracts. *Baghdad Science Journal.* **2020**, *17*(*2*), 670-681. https://doi.org/10.21123/bsj.2020.17.2% 28si%29.0670.
4. Jesús, R.; Reyes-López, A.; Larrañaga, S.Y.; Estévez, M.; Pérez, D.R. Green synthesis of silver nanoparticles using a Melissa officinalis leaf extract with antibacterial properties. *Results in Physics.* **2017**, *7*, 2639-2643. http://dx.doi.org/10.1016/j.rinp.2017.07.044.
5. Al-Saadi, T.M.; Luay, J.k. Preparation of Silver Nanoparticles by Sol-Gel Method and Study their Characteristics. *Ibn AL-Haitham Journal for Pure and Applied Sciences* **2017,** *28*(*1*), 301–310.
6. Jeevanandam, J.; Kiew, S.F.; Boakye-Ansah, S.; Lau, S.Y.; Barhoum, A.; Danquah, M.K.; Rodrigues, J. Green approaches for the synthesis of metal and metal oxide nanoparticles using microbial and plant extracts. *Nanoscale*. **2022**, *14*(*7*), 2534–2571. https://doi.org/10. 1039/d1nr08144f.
7. Quintero-Quiroz, C.; Acevedo, N.; Zapata-Giraldo, J.; Botero Luz, E.; Quintero, J.; Zárate-Triviño, D.; Saldarriaga, J.; Pérez, V.Z. Optimization of silver nanoparticle synthesis by chemical reduction and evaluation of its antimicrobial and toxic activity. *Biomater Research* **2019**, *23*(*27*),23-45. https://doi.org/10.1186%2Fs40824-019-0173-y.
8. Widatalla, H.A.; Yassin, L.F.; Alrasheid, A.A.; Ahmed, S.; Widdatallah, M.O.; Eltilib, S.H.; Mohamed, A.A. Green synthesis of silver nanoparticles using green tea leaf extract, characterization and evaluation of antimicrobial activity. *Nanoscale Advances.* **2022**, *4*(*3*), 911–915. https://doi.org/10.1039/d1na00509j.
9. Rakaa, J.M.; Obaid, A.S. Biosynthesis of silver nanoparticles using Thyme vulgaris leaves extract and its antibacterial activity. *Iraqi Journal of Physics* **2020**, *18*(*46*), 1-12. https://doi.org /10.30723/ijp.v18i46.559.
10. Hammami, I.; Alabdallah, N.M. Gold nanoparticles: Synthesis properties and applications. *Journal of King*

Saud University Science **2021**, *33*, 7, 101560. https://doi.org/10.1016 /J.JKSUS.2021.101560.

11. Padilla-Cruz, A.L.; Garza-Cervantes, J.A.; Vasto-Anzaldo, X.G.; García-Rivas, G.; Buitimea, A.L.; Morones-Ramírez, J.R. Synthesis and design of Ag–Fe bimetallic nanoparticles as antimicrobial synergistic combination therapies against clinically relevant pathogens. *Scientific Reports* **2021**, *11*(*1*), 1-10. https://doi.org/10.1038/s41598-021-84768-8.

12. Adil, B.H.; Al-Shammari, A.M.; Murbat, H.H. Breast cancer treatment using cold atmospheric plasma generated by the FE-DBD scheme. *Clinical Plasma Medicine* **2020**, *19*, 100103. https://doi.org/10.1016/j.cpme.2020.100103.

13. Graves, D.B. The emerging role of reactive oxygen and nitrogen species in redox biology and some implications for plasma applications to medicine and biology. *Journal of Physics D: Applied Physics* **2012**, *45*, 26, 263001. https://doi.org/10.1088/0022-3727%2F45%2F26%_2F263001.

14. Guerrero-Preston, R.; Ogawa, T.; Uemura, M.; Shumulinsky, B.G.; Valle, L.; Pirini, F.; Ravi, R.; Sidransk, D.; Keidar, M.; Trink, B. Cold atmospheric plasma treatment selectively targets head and neck squamous cell carcinoma cells. *International Journal of Molecular Medicine* **2014**, *34*(*4*), 941-946. https://doi.org/10.3892/ijmm.2014.1849.

15. Kong, M.G.; Kroesen, G.; Morfill, G.; Nosenko, T.; Shimizu, T.; Van Dijk, J.; Zimmermann, J. L. Plasma medicine: an introductory review. *New Journal of Physics* **2009**, *11*, 11, 115012. https://doi.org/10.1088/1367-2630%2F11%2F11%2F115012.

16. Graves, D.; Hamaguchi, S.; O'Connell, D. *Biointerphases*. **2015**, *10(2)*, 029301.

17. Khun, J.; Machková, A.; Kašparová, P.; Klenivskyi, M.; Vaňková, E.; Galář, P.; Julák, J.; Scholtz, V. Non-thermal plasma sources based on cometary and point-to-ring discharges. *Molecules*.**2021**, *27(1)*, 238-245. https://doi.org/10.3390/molecules27010238.

18. Mohammed, M.S.; Adil, B.H.; Obaid, A.S.; Al-Shammari, A.M. Plasma Jet Prepared Gold and Silver Nanoparticles to Induce Caspase-Independent Apoptosis in Digestive System Cancers. *In Materials Science Forum* **2022,** *1050*, 51-63. https://doi.org/10.1016/j.cpme.2020.100103.

19. Kaddoori, F.F.; Oleiwi, H.F.; Obaid, A.S.; Al-Ansari, R.A.; Adil, B.H.; Adnan. A.F. The effect of plasma jet-generated gold nanoparticles on liver functions. *In AIP Conference Proceedings* **2022**, *2437*, 1, 020003. https://doi.org/10.1063/5.0092329.

20. Vasudevan, A.; Shvalya, V.; Košiček, M.; Zavašnik, J.; Jurov, A.; Santhosh, N.M.; Zidanšek, A.; Cvelbar, U. From faceted nanoparticles to nanostructured thin film by plasma-jet redox reaction of ionic gold. *Journal of Alloys and Compounds* **2022**, *928,* 167155. https://doi.org/ 10.1016/j.jallcom.2022.167155.

21. Ibrahim, K.; Khalid, S.; Idrees, K. Nanoparticles: Properties, Applications and toxicities. *Arabian Journal of Chemistry* **2019**, *12*, 7, 908-931. https://doi.org/10.1016/j.arabjc.2017.05.011.

22. Norton, K.J.; Firoz, A.; David, J.L.; A review of the synthesis, properties, and applications of bulk and two-dimensional tin (II) sulfide (SnS). *Applied Sciences* **2021,** *11*, 5, 2062. https://doi.org /10.3390/app11052062.

23. Yu, J.; Yingeng, W.; Yan, H.; Xiuwen, W.; Jing, G.; Jingkai, Y.; Hongli, Z. Structural and electronic properties of SnO_2 doped with non-metal elements. *Beilstein Journal of Nanotechnology* **2020,** *11*(*1*), 1321-1328. https://doi.org/10.3762/bjnano.11.116.

24. Pargoletti, E.; Umme, H.H.; Iolanda, D.B.; Hongjun, C.; Thanh, T.P.; Gian, L.; Chiarello, J.; Lipton, D.; Valentina, P.; Antonio, T.; Giuseppe, C. Engineering of SnO_2–graphene oxide nano heterojunctions for selective room-temperature chemical sensing and optoelectronic devices. *ACS Applied Materials & interfaces* **2020,** *12*(*35*), 39549-39560. https://doi.org/10.1021/acsami. 0c09178.

25. Wang, B.; Zhu, L.F.; Yang, Y.H.; Xu, N.S.; Yang, G.W. Fabrication of a SnO2 nanowire gas sensor and sensor performance for hydrogen. *The Journal of Physical Chemistry C.* **2008,** *112*(*17*), 6643-6647. https://doi.org/10.1021/jp8003147.

26. Das, S.; Jayaraman, V. SnO_2: A comprehensive review on structures and gas sensors. *Progress in Materials Science* **2014,** *66,* 112-255. https://doi.org/10.1016/j.pmatsci. 2014.06.003.

27. Castro, A.; Marques, M.A.; Rubio, A. Propagators for the time-dependent Kohn–Sham equations. *The Journal of Chemical Physics* **2004**, *12*(*8*), 3425-33. https://doi.org/10. 1063/1.1774980.

28. Brockherde, F.; Vogt, L.; Li, L.; Tuckerman, M.E.; Burke, K.; Müller. K.R. Bypassing the Kohn-Sham equations with machine learning. *Nature Communications* **2017**, *8*, 1, 872. https://doi.org /10.1038/s41467-017-00839-3.

29. Sahoo, L.; Bhuyan, S.; Das, S.N. Structural, morphological, and impedance spectroscopy of Tin oxide-Titania based electronic material. *Physica B: Condensed Matter* **2023,** 654, 414705. https://doi.org/10.1016/j.physb.2023.414705.

30. Tui, R.; Sui, H.; Mao, J.; Sun, X.; Chen, H.; Duan, Y.; Yang, P.; Tang, Q.; He, B. Round-comb Fe_2O_3& SnO_2 heterostructures enable efficient light harvesting and charge extraction for high-performance all-inorganic perovskite solar cells. *Journal of Colloid and Interface Science* **2023**, *15,* 640, 18-27. https://doi.org/10.1016/j.jcis.2023.03.034.

31. Du, B.; Kun, He.; Gangqi, T.; Xiang, C.; Lin, S. Robust Electron Transport Layer of SnO_2 for Efficient Perovskite Solar Cells: Recent Advances and Perspectives. *Journal of Materials Chemistry C.* **2023**, *12*, 3. http://dx.doi.org/10.1016/j.optmat.2023.113518.